Original Article

Three-dimensional assessment of the middle cranial fossa and central skull base following Herbst appliance treatment

Karine Sayure Okano[a]; Lucia Helena Soares Cevidanes[b]; Paula Loureiro Cheib[c]; Antonio Carlos de Oliveira Ruellas[d]; Marília Yatabe[e]; Tung Nguyen[f]; Lorenzo Franchi[g]; James A. McNamara Jr.[h]; Bernardo Quiroga Souki[i]

ABSTRACT

Objectives: The purpose of this three-dimensional (3D) study was to assess retrospectively the middle cranial fossa and central skull base of patients treated with the Herbst appliance (HA).

Materials and Methods: 3D surface virtual models of 40 Class II, division 1 malocclusion patients were generated from cone-beam computed tomography (CBCT) acquired before treatment (T0) and after 8 months of HA treatment (T1). T0 and T1 3D models were superimposed volumetrically at the anterior cranial fossa. Twenty subjects who had been treated with the Herbst appliance (HAG) were compared to 20 subjects who were not treated orthopedically. The latter group served as a comparison control group (CG). Quantitative assessments of the location and directional changes were made with linear and angular measurements between anatomical landmarks. Qualitative assessments of the spatial behavior of the middle cranial fossa and central skull base relative to the anterior cranial fossa were displayed graphically for visualization with color maps and semitransparent overlays. Non-parametric tests were performed to compare the between the HAG and CG.

Results: Point-to-point linear measurements and skeletal rotation (pitch, roll, and yaw) changes were very small along the observational period and were not significantly different between HAG and CG. Visual analysis of color maps and overlays confirmed that no changes in the cranial base were associated with HA.

Conclusions: HA therapy did not produce clinically significant changes in the middle cranial fossa and central skull base. (*Angle Orthod.* 2018;88:757–764.)

KEY WORDS: Middle cranial fossa; Central skull base; Angle Class II malocclusion; Computed tomography; Three-dimensional imaging

[a] Resident, Graduate Program in Orthodontics, Pontifical Catholic University of Minas Gerais, Belo Horizonte, Minas Gerais, Brazil.

[b] Assistant Professor, Department of Orthodontics and Pediatric Dentistry, School of Dentistry, University of Michigan, Ann Arbor, Mich, USA.

[c] PhD student, Graduate Program in Orthodontics, Pontifical Catholic University of Minas Gerais, Belo Horizonte, Minas Gerais, Brazil.

[d] Associate Professor, Department of Orthodontics, Federal University of Rio de Janeiro, Rio de Janeiro, Brazil.

[e] PhD student, Department of Orthodontics, School of Dentistry, University of Sao Paulo, Sao Paulo, Brazil.

[f] Assistant Professor, Department of Orthodontics, School of Dentistry. University of North Carolina, Chapel Hill, NC, USA.

[g] Assistant Professor, Department of Surgery and Translational Medicine, University of Florence School of Dentistry, Florence, Italy.

[h] Graber Endowed Professor Emeritus, Department of Orthodontics and Pediatric Dentistry, University of Michigan, Ann Arbor, Mich, USA.

[i] Associate Professor, Department of Orthodontics, Pontifical Catholic University of Minas Gerais, Belo Horizonte, Minas Gerais, Brazil.

Corresponding author: Dr Bernardo Quiroga Souki, Avenida Dom José Gaspar, 500, Coração Eucarístico, Belo Horizonte, MG 30535-901, Brazil
(e-mail: souki.bhe@terra.com.br)

INTRODUCTION

The Herbst appliance (HA) has gained popularity among orthodontists[1] because it consistently has proven to be a clinically effective and efficient device in improving Class II sagittal discrepancy and enhancing mandibular advancement.[2,3] At this point, there is evidence relative to the dentoalveolar, facial, and skeletal effects of the Herbst appliance,[4–6] but no previous study has considered treatment-related changes and side effects in the position and morphology of the cranial base associated with HA treatment.

It may be speculated that, with the mandibular forward and downward displacement created by HA insertion, the glenoid fossae located in the temporal bone experiences traction in an anterior and inferior direction. Moreover, the styloid processes of the temporal bone are loaded with the stretching of the stylomandibular ligament that limits movements of the mandible anteriorly. As muscular traction that applies continuous forces over a long period of time can cause direct and indirect skeletal changes,[7] the middle cranial fossa, which consists of the sphenoid bone and the two temporal bones, also may undergo traction in an anterior and inferior direction after HA insertion.

Regarding the central skull base, there is histological evidence of mechanical stimulation, as traction forces applied to the spheno-occipital synchondrosis may induce and potentiate growth.[8] Thus, there is a chance, at least theoretically, that changes in that region also might occur associated with HA insertion.

Methodological assessment of these changes, however, is a challenge using conventional imaging methods. Two-dimensional (2D) evaluation of the cranial base using lateral cephalometric radiographs has had limited usefulness because of the overlap of multiple structures, distortion of images, and difficulty in identifying anatomical landmarks accurately, thus generating observer-dependent bias.[9] But, with improvement of three-dimensional (3D) imaging methods, such evaluation is now possible. Using voxel-based volumetric registration, a fully-automated superposition in the anterior cranial fossa is possible, reducing the systematic errors and limitations inherent to 2D imaging techniques.[10]

The objective of the current study was to perform a 3D CBCT assessment of the middle cranial fossa and central skull base of Class II division 1 malocclusion patients treated with the Herbst appliance, comparing the positional and morphological changes to a matched group of patients not undergoing functional jaw orthopedics.

MATERIALS AND METHODS

This study was approved by Institutional Review Board of the Pontifical Catholic University of Minas Gerais, Belo Horizonte, Brazil. From the database of patients treated with HA at the Pontifical Catholic University of Minas Gerais, a sample of patients was selected for this retrospective evaluation (HAG). Based on data collected from 10 randomly selected patients, the sample size was calculated (n = 20 individuals for each group), taking into account a standard deviation of 0.54 mm (basion displacement, the primary outcome of the investigation), an alpha significance level of 0.05, and a beta of 0.2 to achieve 80% power to detect morphological changes in the base of the posterior skull with the minimum detectable difference of 0.5 mm. The effect size was 0.92. Also from the same university database, the comparison group (CG) consisted of patients who were candidates for HA therapy but who required previous additional dental or orthodontic treatment. Thus, the sample consisted of 40 adolescents with Class II division 1 malocclusion, ranging from 12 to 16 years of age, 20 in the HAG (mean age 13.8 ± 1.2 years) and 20 in the CG (mean age 14.4 ± 0.9 years).

At the beginning of the study (T0), all patients had Class II/1 skeletal malocclusion (ANB $\geq 4°$), a convex profile, were in the permanent dentition, and a clinically diagnosed mandibular retrusion. The amount of overjet in the HAG patients allowed a full activation of the appliance in order to correct the malocclusion. However, the amount of sagittal and vertical activation varied among patients.

All patients had active growth potential (CS3-CS4) as determined according to the cervical vertebral maturation method[11] and also had a need for orthodontic treatment. The study excluded individuals who had syndromes, clefts, dentofacial deformities, or temporomandibular joint dysfunction as well as individuals who had undergone previous treatment with functional appliance therapy.

Image Acquisition

In the HAG, CBCTs were acquired before appliance insertion (T0) and at the end of functional treatment (T1) 8 months later. In the CG, CBCTs were acquired at the beginning of the study (T0), and approximately 8 to 12 months later (T1). CBCTs were acquired with an i-CAT scanner (Imaging Sciences International, Hatfield, Pennsylvania, USA) with FOV of 16 cm × 22 cm view, voxel of 0.3 × 0.3 × 0.3 mm, 36.90 mA 120kV and 40 seconds of exposure. All patients were instructed to bite into maximum intercuspation during CBCT acquisition. Verification of condylar seating in the glenoid fossa was verified for each CBCT scan.
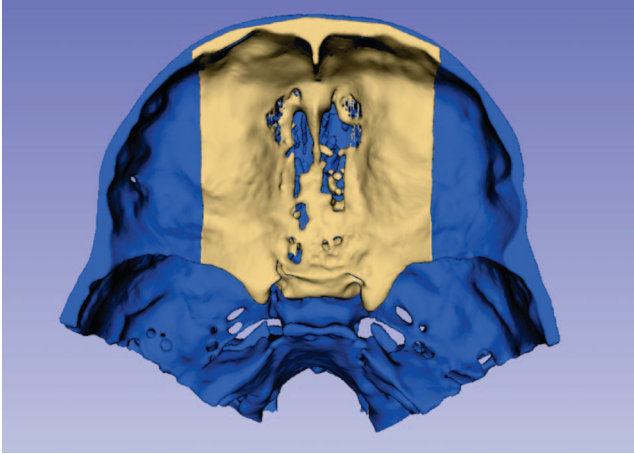
Figure 1. 3D mask of the anterior cranial fossa used as the fiduciary region for the volumetric superimposition of T1 and T0 CBCTs.

Image Analyses

Scans were subjected to 3D analysis using open-source ITK-SNAP software version 2.2 (open-source, www.itksnap.org), and open-source 3D Slicer CMF version 3.0 (open-source, www.slicer.org). Analysis was undertaken in five steps: (1) construction of 3D surface virtual models of the head of each patient or subject; (2) orientation of the head in the same Cartesian coordinate system; (3) manual approximation, and subsequent automated voxel-based volumetric registration of scans and label maps (3D superposition) using a 3D mask of the anterior cranial fossa (Figure 1); (4) identification of the anatomic landmarks (Figure 2); and (5) quantitative measurements and visual analysis, using point-to-point measurements and semitransparent overlays of the 3D virtual models.

Identification of the Anatomic Landmarks

Anatomic landmarks located in the middle cranial fossa and in the central skull base (Figure 2) were identified in the multi planar coronal, sagittal, and axial views, as illustrated in Figure 3, and were prelabeled with a 0.5 mm spherical dots.[12] The following landmarks were selected: S1 (floor of sella turcica, or sella inferior), S2 (posterior wall of sella turcica, or sella posterior), S3 (superior-posterior point of the sella turcica, or clinoid process), SO (most superior-anterior point of the occipital bone in the junction of the spheno-occipital synchondrosis), B (Basion), SPL (inferior point of the left side styloid process), SPR (inferior point of the right-side styloid process), GFL (most superior point of the left-side glenoid fossa), and GFR (most superior point of the right-side glenoid fossa)

## Quantitative Evaluation and Visual Analysis

Quantitative evaluation of the changes of the cranial base was performed by measuring the point-to-point displacement using the Q3DC tool of 3D Slicer software (Figure 4). Visual analytics also were performed with 3D Slicer, using semitransparent overlays
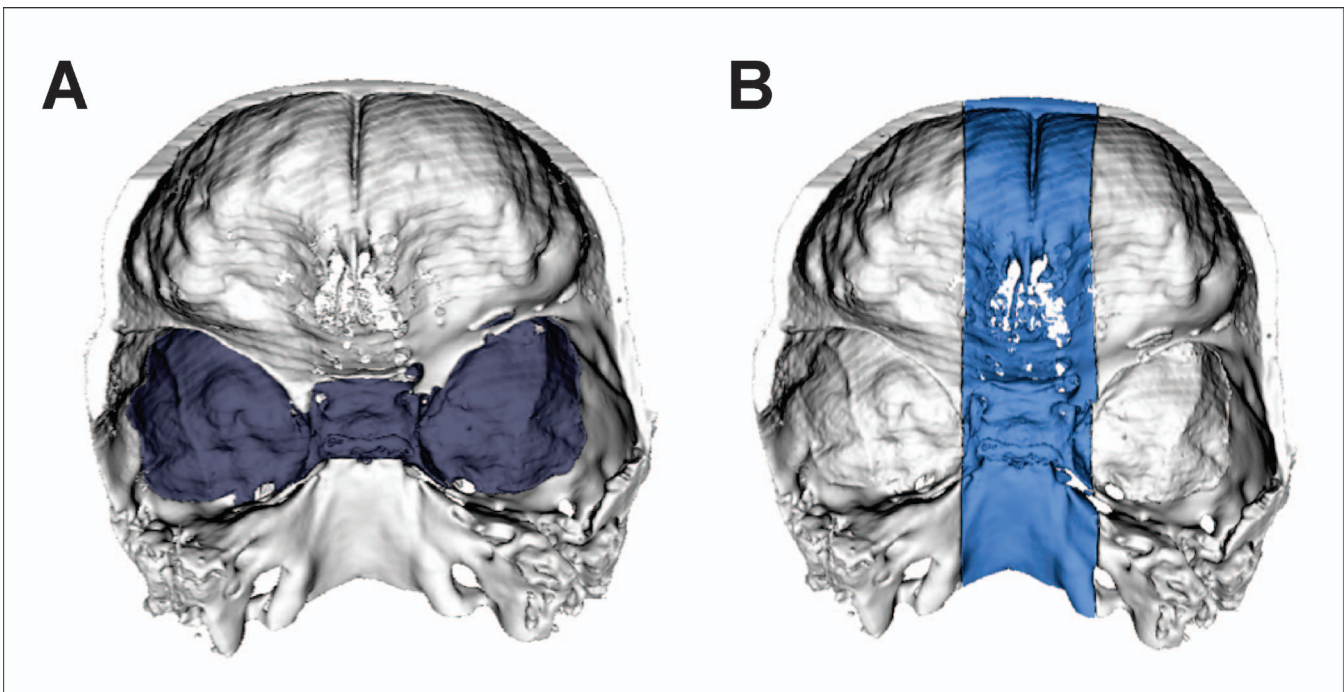
Figure 2. Anatomic boundaries of the middle cranial fossa (A) and central skull base (B).
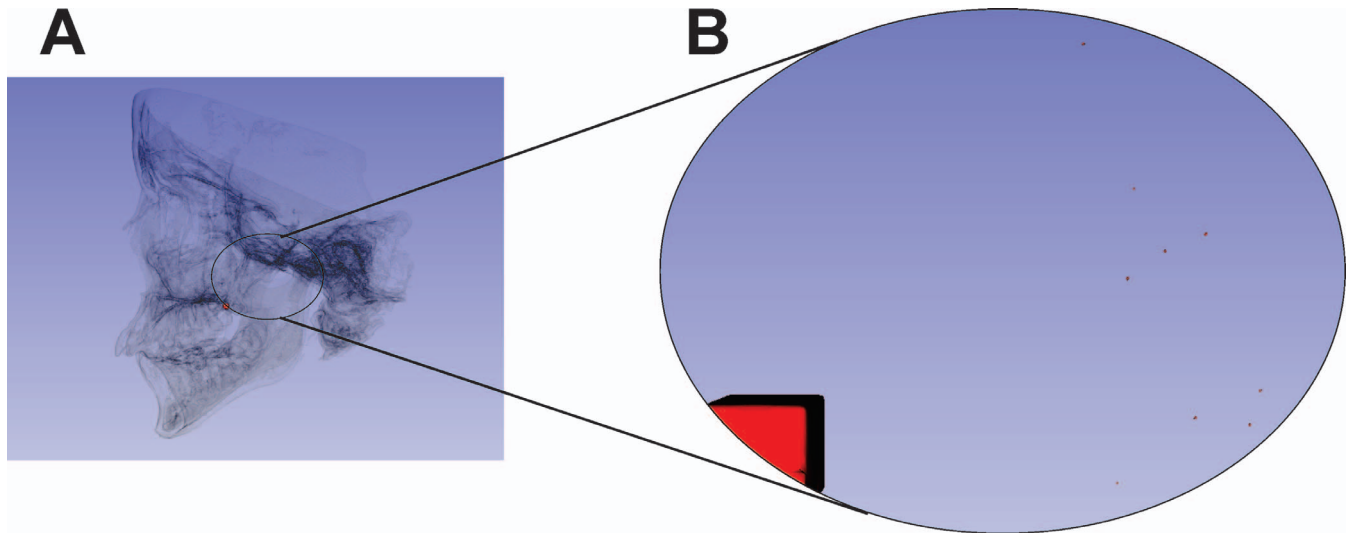
Figure 3. (A) 3D virtual model with 0.5 mm spherical landmarks (so small that they cannot be seen in this full head view), and 5 mm square spatial positioning reference locator. (B) Close-up view, showing the 0.5 mm spherical landmarks, and section of the square reference locator.

(Figure 5) that were associated with the closest-point color-mapping (Figure 6).

Displacements were evaluated as the linear projection in the multiplanar 2D Cartesian coordinates (X, Y, and Z). The 2D linear projection of the anterior-posterior displacement ($\triangle$Y) and the inferior-superior displacement (ΔZ) were measured in the sagittal plan (YZ); the right-left 2D linear displacement ($\triangle$X) was measured in the axial plane (XY). The rotation (pitch, roll, and yaw) of the posterior region of the cranial base also was measured in the three planes of space. Pitch was measured as the angular changes of the S1-Ba

line between T0 and T1 in sagittal view. Roll was measured as the angular changes of the SPR-SPL and GFR-GFL lines between T0 and T1 in a coronal view. Yaw was measured as the angular changes SPR-SPL and GFR-GFL lines in the axial perspective.

Statistical Analysis

Data analysis was performed using SPSS (version 20.0; SPSS, Chicago, Ill). Intra- and interobserver agreement was tested using intraclass correlation coefficient (ICC). Ten randomly selected patients were remeasured by one investigator (KSO) after a 2-week interval; the same patients were also measured by a
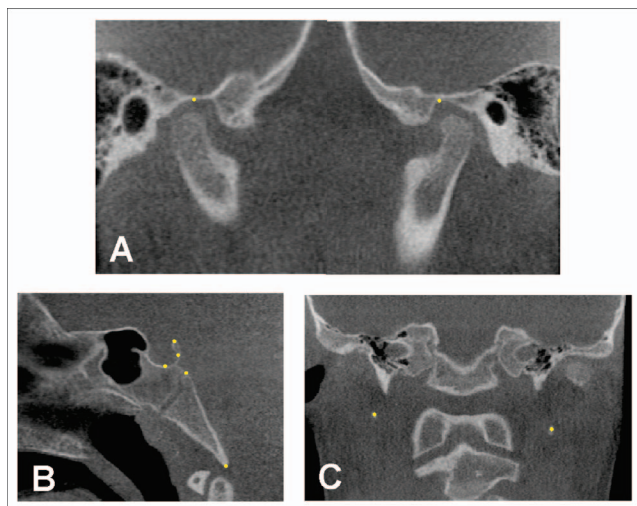
Figure 4. Landmarks. (A) Mid-sagittal view: S1-Sella inferior; S2-Sella posterior; S3–Clinoid process; SO–Occipital bone at the superior aspect of the spheno-occipital synchondrosis; B–Basion; (B) Para-sagittal view: GFL-Glenoid fossa left; GFR-Glenoid fossa right. (C) Coronal view: SPL-Styloid process left; SPR-Styloid process right.
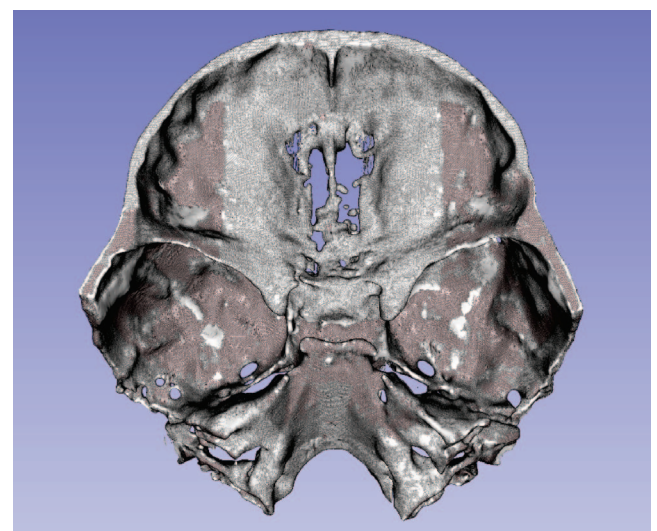
Figure 5. Semitransparent overlay of two-time point 3D virtual models (T0 and T1). White color indicates the perfect matching of the T0 and T1 models, while darker regions indicate changes in the position and or morphology of the T1 model relative to the T0 model.
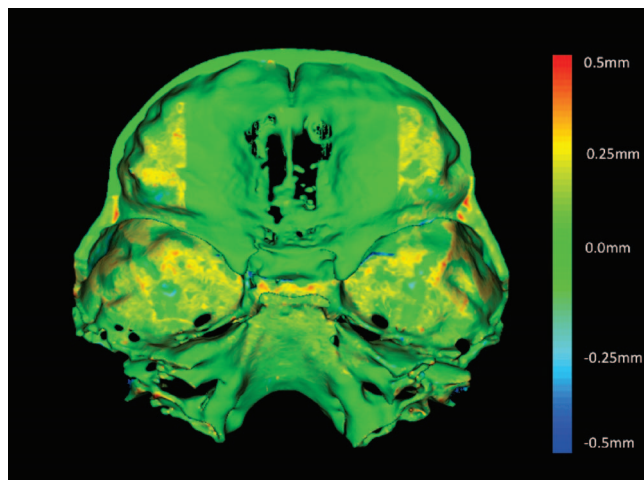
Figure 6. Closest-point color mapping of distances of the T1 and T0 models. Green color indicates no displacement between models. Red is 0.5 mm displacement, light blue is −0.5 mm displacement of T1 relative to T0 model.

second investigator (BQS). Systematic error and random error assessments were performed with a paired *t*-test and method of moments' estimator,[13] respectively. The assumptions of normality and same variance were not met. Therefore, non-parametric statistical analysis with the Mann-Whitney *U*-test to compare the differences between HAG and CG was employed.

RESULTS

ICCs were greater than 0.80, showing an adequate reproducibility and repeatability. Quantitative evaluation of changes in the cranial base is reported in Tables 1 and 2. Negative values indicate downward, to the left, and clockwise rotation, while positive values indicate upward, to the right, and counterclockwise rotation.

Table 1 shows the linear displacement of the temporal and occipital bone between T0 and T1 in the projected X, Y, Z, and Euclidean 3D. Except for the anterior-posterior displacement (Y projection) and inferior-superior displacement (Z projection) of the point located in the lower region of sella turcica, and the inferior-superior displacement (Z projection) of basion, all variables describing point displacements did not show statistically significant differences between HAG and CG ($P > .05$). Moreover, the mean differences between HAG and CG were all equal to or smaller than 0.5 mm.

Rotational changes of the posterior region of the cranial base, measured as pitch, roll, and yaw, are described in Table 2. No significant differences were observed in the HAG compared to the CG ($P > .05$). Additionally, the rotational difference between HAG and CG were equal to or smaller than 0.5°.

Figure 5 shows the semitransparent overlay of the two-time point (T0 and T1) virtual models of an HAG patient. The predominance of white color in the anterior cranial fossa indicates the perfect matching of the two models with the volumetric superimposition. The darker region around the anterior fossa indicates some morphological or positional change at T1 relative to T0. The magnitude of this change can be visualized with the color-maps (Figure 6). The color range scale was set at 0.5 mm.

DISCUSSION

This study is the first report to investigate directly whether changes occur in the cranial base during therapy with a fixed functional appliance. In theory, some sort of positional or morphological change in the cranial base might be expected, especially the displacement of the temporal bone and of the central skull base region (clivus region), in that strong forces are applied indirectly as a result of stretching the temporomandibular joint ligaments of the articular capsule and mandibular ligaments during therapeutic chin advancement.

In the current study, quantitative assessments and 3D visual analysis of the cranial base region following HA treatment were possible only because new imaging analysis tools have become available recently. This voxel-based method offers advantages over the 2D method because this analytical approach utilizes thousands of voxels rather than a limited number of landmarks and also is not observer-dependent. Although cephalograms have contributed to the understanding of facial growth for decades, the use of lines, planes, and points as references has limited capacity to offer a reliable way for a longitudinal 3D assessment. Additionally, prior to the introduction of 3D methods, the study of roll and yaw facial rotations was limited to PA and submentovertex cephalograms. This approach limited the comprehension of possible cranial deflections with growth and response to treatment in three dimensions, particularly during the pubertal growth spurt.

The literature is consistent with the belief that growth of the spheno-occipital synchondrosis is associated strongly with the growth of the cranial base and that its full maturation occurs long after puberty.[14] In addition, rotational changes in the cranial base, as indicated by the deflection of the occipital bone relative to the anterior cranial base, may result from bone remodeling during pubertal growth.[15] As the evaluation of growth changes in the craniofacial complex is performed relative to reference structures, the measurements in this study were performed using the anterior cranial fossa as the structure of reference for superimposition

Table 1. Comparison of the X, Y, Z, and 3D Changes of Sphenoid (Sella Turcica), Occipital (Spheno-Occipital Synchondrosis and Basion), and Temporal Bones (Glenoid Fossae and Styloid Processes) Between Pretreatment (T0) and Posttreatment (T1)[a]

Measurements	Coordinates	Groups	Mean	SD	Median	25th	75th	Diff Means	P Value
Sella inferior	x	CG	0.00	0.04	0.00	0.01	0.03		.565
		HAG	−0.01	0.05	0.00	−0.04	0.03	0.01	
	y	CG	−0.30	0.42	−0.30	−0.59	0.00		.033*
		HAG	−0.01	0.39	0.02	−0.28	0.27	0.29	
	z	CG	−0.02	0.41	−0.15	−0.29	0.27		.004*
		HAG	0.31	0.36	0.27	0.14	0.45	0.33	
	3D	CG	0.58	0.29	0.51	0.35	0.79		.327
		HAG	0.51	0.32	0.37	−0.31	0.66	0.06	
Sella posterior	x	CG	−0.02	0.07	0.00	−0.07	0.03		.221
		HAG	0.01	0.04	0.00	−0.01	0.03	0.03	
	y	CG	−0.25	0.39	−0.14	−0.32	−0.01		.289
		HAG	−0.11	0.35	−0.03	−0.51	0.24	0.14	
	z	CG	0.02	0.45	−0.15	−0.23	0.13		.086
		HAG	0.18	0.39	0.16	−0.11	0.45	0.16	
	3D	CG	0.49	0.42	0.32	0.23	0.51		.174
		HAG	0.49	0.27	0.49	0.36	0.62	0.00	
Clinoid process	x	CG	−0.01	0.07	0.00	0.61	0.04		.565
		HAG	−0.01	0.09	−0.01	−0.06	0.04	0.00	
	y	CG	−0.34	0.37	−0.30	−0.58	−0.05		.114
		HAG	−0.14	0.42	0.00	−0.46	0.08	0.20	
	z	CG	0.09	0.34	0.10	−0.13	0.36		.398
		HAG	0.27	0.54	0.18	−0.12	0.56	0.18	
	3D	CG	0.52	0.33	0.47	0.32	0.69		.620
		HAG	0.60	0.45	0.52	0.33	0.85	0.08	
Spheno-occipital Synchondrosis	x	CG	−0.01	0.07	0.00	−0.06	0.05		.947
		HAG	0.00	0.06	0.00	−0.06	0.06	0.00	
	y	CG	−0.14	0.48	−0.08	−0.34	0.02		.277
		HAG	−0.40	0.57	−0.25	−0.82	−0.01	0.26	
	z	CG	−0.03	0.57	−0.03	−0.53	0.34		.221
		HAG	0.20	0.62	0.35	−0.42	0.73	0.23	
	3D	CG	0.63	0.40	0.56	0.33	0.78		.056
		HAG	0.85	0.42	0.75	0.47	1.07	0.21	
Basion	x	CG	−0.61	0.65	−0.49	−1.01	−0.22		.547
		HAG	−0.57	0.87	−0.38	−1.36	0.53	0.03	
	y	CG	−0.01	0.05	0.00	−0.06	0.04		.142
		HAG	0.02	0.06	0.00	−0.04	0.07	0.04	
	z	CG	−0.29	0.51	−0.19	−0.61	0.06		.001*
		HAG	0.23	0.47	0.27	−0.11	0.55	0.52	
	3D	CG	0.89	0.57	0.64	0.43	1.23		.925
		HAG	0.92	0.69	0.75	0.36	1.43	0.03	
Glenoid Fossa Left	x	CG	−0.31	0.55	−0.3	−0.69	0.02	0.06	.820
		HAG	−0.25	0.7	−0.27				
	y	CG	−0.27	0.64	−0.05	−0.8	0.17	0.22	.277
		HAG	−0.05	0.76	0.02				
	z	CG	0.01	0.44	−0.03	−0.24	0.35	0.06	.738
		HAG	0.07	0.66	0.00				
	3D	CG	0.93	0.42	0.87			0.11	.495
		HAG	1.08	0.6	0.88				
Glenoid Fossa Right	x	CG	−0.35	0.64	−0.33	−1.04	0.25	0.09	.583
		HAG	−0.24	0.60	−0.05				
	y	CG	0.45	0.78	0.30	−0.03	0.89	0.11	.862
		HAG	0.34	0.94	0.48				
	z	CG	−0.05	0.41	0.03	−0.28	0.18	0.08	.478
		HAG	0.03	0.50	0.11				
	3D	CG	1.10	0.51	1.09	0.62	1.31	0.01	.904
		HAG	1.11	0.61	1.15				

 [a] SD indicates standard deviation; 25th, 25th percentile; 75th, 75th percentile; Diff Means, difference between means; X, Right-Left; Y, Anterior-Posterior; Z, Inferior-Superior; 3D, Euclidean distance.

Table 2. Descriptive Data and Statistical Analysis of the Comparison of the Angular Changes Between Pretreatment (T0) and Posttreatment (T1) in the Comparison Group (CG) and Herbst Appliance Group (HAG)[a,b]

Measurements	Coordinates	Groups	Mean	SD	Median	P Value
Sella turcica - Basion	Pitch	CG	−0.18	0.94	−0.24	.231
		HAG	−0.55	0.64	−0.54	
Styloid process L - Styloid proces R	Yaw	CG	0.28	1.14	0.08	.773
		HAG	0.22	0.79	−0.03	
	Roll	CG	−0.37	1.74	−0.25	.686
		HAG	−0.06	0.45	−0.01	
Glenoid fossa L - Glenoid fossa R	Yaw	CG	−0.02	0.33	0.06	.698
		HAG	0.02	0.48	0.11	
	Roll	CG	−0.03	0.23	0.01	.529
		HAG	−0.03	0.37	−0.13	

[a] positive values indicate clockwise rotation; negative values indicate counterclockwise rotation.
[b] R indicates right; L, left.

based on the assumption proposed by Björk[16] that the anterior cranial fossa is a stable reference during puberty.

Patients in the current sample were all growing individuals, with 36 of the patients showing an open spheno-occipital synchondrosis; only four had completely fused synchondroses. However, large variability was observed in the degree of maturation of the spheno-occipital synchondrosis. Although some patients had a completely open spheno-occipital synchondrosis, in other patients at the same stage of cervical vertebral skeletal maturation (CVM), the spheno-occipital synchondrosis was completely or almost completely fused. According to a recently proposed method of scoring the stages of synchondrosis fusion,[14] patients in the current sample had the following pattern of maturation: eight patients in Stage 1, seven in Stage 2, eight in Stage 3, 12 in Stage 4, and four patients in Stage 5. However, the association between CVM and synchondrosis maturation was not found, as reported previously.[14] The explanation for such variability in synchondrosis maturation in these 12- to 16-year-old patients can be found by the conclusions presented by Melsen,[17] who found that the age of complete fusion of the spheno-occipital synchondrosis is variable, occurring by 16 to 17 years of age in women and at 18 to 19 years in men.

Ford[18] commented that, in some individuals, the spheno-occipital synchondrosis might continue to grow until the age of 20 to 25 years of age. In a recent study using 3D images, Sinanoglu et al.[19] showed that the mean age for complete fusion of the spheno-occipital synchondrosis was 18 and 20 years for women and men, respectively. Regardless of the degree of maturity of the spheno-occipital synchondrosis, after the analysis of 40 patients with growth between 12 and 16 years of age, 20 in the treated group and 20 in the comparison group, the current data showed that there were no visual or clinically significant changes (the color-mapping scale was set to identify differences greater than 0.5 mm) in the three planes of space in the posterior region of the cranial base relative to the anterior cranial fossa. Recently, Stepanko and Lagravère[20] reported no clinically significant changes in the sphenoid bone due to rapid maxillary expansion treatments regardless of gender or treatment type, which is in agreement with the evidence collected in the current investigation.

In this study, most of the measurements did not show statistically significant differences in displacements and rotations between the treated and comparison groups. Only four measurements showed statistically significant differences between the two groups, but these differences were not clinically significant. For those variables, the mean differences between the two groups were very small, ie, within the computer margin of error of landmark selection (0.5 mm), or the voxel size (0.3 mm).

As intra-and interobserver variability in landmark placement can occur, affecting the repeatability and reproducibility of measurement; in the current investigation 3D-CBCT cephalometric landmarks with high reliability were chosen.[21] ICC showed high intra- and interobserver agreement between readings. In the qualitative assessment with the semitransparent overlays and color-maps, it was possible to visualize the entire cranial base, confirming the quantitative findings.

Based on the current dataset, it seems clear that the load generated by the HA on the glenoid fossa region after forced mandibular advancement does not appear to alter the amount or direction of growth of the middle cranial base fossa or the central skull base.

CONCLUSIONS

• There were no positional or morphological changes in the cranial base associated with the use of the Herbst appliance.

REFERENCES

1. Silva JFE, Gerszewski C, Moresca RC, Correr GM, Flore-Mir C, Moro A. Retrospective study of clinical complications during orthodontics treatment with either a removable mandibular acrylic splint Herbst or with a cantilever Herbst. *Angle Orthod*. 2015;85(1):64–71.

2. Cozza P, Baccetti T, Franchi L, De Toffol L, McNamara JA Jr. Mandibular changes produced by functional appliances in Class II malocclusion: a systematic review. *Am J Orthod Dentofacial Orthop*. 2006;129:599e1–599e12.

3. Yang X, Zhu Y, Long H, et al. The effectiveness of the Herbst appliance for patients with Class II malocclusion: a meta-analysis. *Eur J Orthod*. 2016;38:324–333.

4. Souki BQ, Vilefort PLC, Oliveira DD, et al. Three-dimensional skeletal mandibular changes associated with Herbst appliance treatment. *Orthod Craniofac Res*. 2017;20:111–118.

5. Rego MV, Martinez EF, Coelho RMI, Leal LMP, Thiesen G. Perception of changes in soft-tissue profile after Herbst appliance treatment of Class II Division 1 malocclusion. *Am J Orthod Dentofacial Orthop*. 2017;151:559–564.

6. Perinetti G, Primožič J, Furlani G, Franchi L, Contardo L. Treatment effects of fixed functional appliances alone or in combination with multibracket appliances: a systematic review and meta-analysis. *Angle Orthod*. 2015;85:480–492.

7. Moss ML. The functional matrix hypothesis revisited. 2. The role of an osseous connected cellular network. *Am J Orthod Dentofacial Orthop*. 1997;112:221–226.

8. Lei WY, Wong RWK, Rabie ABM. Factors regulating endochondral ossification in the spheno-occipital synchondrosis. *Angle Orthod*. 2008;78:215–220.

9. Durão AR, Pittayapat P, Rockenbach MIB, et al. Validity of 2D lateral cephalometry in orthodontics: a systematic review. *Prog Orthod*. 2013;14:31–41.

10. Cevidanes LHC, Heymann G, Cornelis MA, et al. Superimposition of 3-dimensional cone-beam computed tomography models of growing patients. *Am J Orthod Dentofacial Orthop*. 2009;136:94–99.

11. Baccetti T, Franchi L, McNamara JA Jr. The Cervical Vertebral Maturation (CVM) method for the assessment of optimal treatment timing in dentofacial orthopedics. *Sem Orthod*. 2005;11:119–129.

12. Ruellas AC, Yatabe MS, Souki BQ, et al. 3D mandibular superimposition: comparison of regions of reference for voxel-based registration. *PLoS One*. 2016; 23:11:e0157625.

13. Springate SD. The effect of sample size and bias on the reliability of estimates of error: a comparative study of Dahlberg's formula. *Eur J Orthod*. 2012;34:158–163.

14. Fernández-Pérez MJ, Alarcón JA, McNamara JA Jr, et al. Spheno-occipital synchondrosis fusion correlates with cervical vertebrae maturation. *PLoS One*. 2016;11:e0161104.

15. Graber LW, Vanarsdall RL, Vig KWL. Orthodontics: Current Principles and Techniques. 5th ed. Philadelphia: Elsevier, Mosby; 2012;8:215–246.

16. Björk A. The use of metallic implants in the study of facial growth in children: method and application. *Am J Phys Anthrop*. 1968;29:243–254.

17. Melsen B. The cranial base: the postnatal development of the cranial base studied histologically on human autopsy material. *Am J Orthod*. 1974;66:689–691.

18. Ford EHR. Growth of the human cranial base. *Am J Orthod*. 1958;44:498–506.

19. Sinanoglu A, Kocasarac HD, Noujeim M. Age estimation by an analysis of spheno-occipital synchondrosis using cone-beam computed tomography. *Legal Medicine*. 2016;18:13–19.

20. Stepanko LS, Lagravère MO. Sphenoid bone changes in rapid maxillary expansion assessed with cone-beam computed tomography. *Korean J Orthod*. 2016;46:269–279.

21. Lisboa C de O, Masterson D, da Motta AF, Motta AT. Reliability and reproducibility of three-dimensional cephalometric landmarks using CBCT: a systematic review. *J Appl Oral Sci*. 2015;23:112–119.